PorSignDB: a database of *in vivo* perturbation signatures for dissecting clinical outcome of PCV2 infection

Nicolaas Van Renne[1¶*], Ruifang Wei[1¶], Nathalie Pochet[2,3], Hans J. Nauwynck[1]

[1]Laboratory of Virology, Faculty of Veterinary Medicine, Ghent University, [2]Ann Romney Center for Neurologic Diseases, Department of Neurology, Brigham and Women's Hospital, Harvard Medical School; [3]Broad Institute of Harvard and Massachusetts Institute of Technology.

¶These authors contributed equally

[*]Corresponding author:

Nicolaas Van Renne

Tel.: +32 489 94 95 39

Email: nicolaas.vanrenne@ugent.be

Abstract

Porcine Circovirus Type 2 (PCV2) is a pathogen that has the ability to cause often devastating disease manifestations in pig populations with major economic implications. How PCV2 establishes subclinical persistence and why certain individuals progress to lethal lymphoid depletion remain to be elucidated. Here we present PorSignDB, a gene signature database describing *in vivo* porcine tissue physiology that we generated from a large compendium of *in vivo* transcriptional profiles and that we subsequently leveraged for deciphering the distinct physiological states underlying PCV2-affected lymph nodes. This systems biology approach indicated that subclinical PCV2 infections shut down the immune system. A robust signature of PCV2 disease emphasized that immune activation is dysfunctional in subclinical infections, however, in contrast it is promoted in PCV2 patients with clinical manifestations. Functional genomics further uncovered IL-2 as a driver of PCV2-mediated disease and we identified STAT3 as a druggable PCV2 host factor candidate. Our systematic dissection of the mechanistic basis of PCV2 reveals that subclinical and clinical PCV2 display two diametrically opposed immunotranscriptomic recalibrations that represent distinct physiological states *in vivo*, which suggests a paradigm shift in this field. Finally, our PorSignDB signature database is publicly available as a community resource (http://www.vetvirology.ugent.be/PorSignDB/, included in Gene Sets from Community Contributors http://software.broadinstitute.org/gsea/msigdb/contributed_genesets.jsp) and provides systems biologists with a valuable tool for catalyzing studies of human and veterinary disease.

Author Summary

Porcine Circovirus Type 2 (PCV2) is a small but economically important pathogen circulating endemically in pig populations. Although PCV2 causes mostly chronic subclinical infections, many individuals develop a lethal form of circoviral disease consisting of a collapse of lymphoid tissue. In order to provide a fresh look at how PCV2 reprograms host tissue, we

created PorSignDB, a compendium of hundreds of transcriptomic gene-expression signatures derived from primary porcine tissue specimens of well over 1500 patients or lab animals. By leveraging PorSignDB on transcriptomic data of PCV2 patients, we uncover that subclinical PCV2 reprograms the host into a striking state of non-infection, which explains its failure to respond to an initial phase of circoviral presence. A PCV2 disease signature further demonstrates that the silenced immune system associated with subclinical PCV2 becomes fully activate in PCV2 patients, triggering severe circoviral disease. Further genomic and functional analysis demonstrate STAT3 as a druggable host factor and IL-2 as a disease driver. Together, this study demonstrates the mechanistic underpinnings of clinical outcome of PCV2 infections: subclinical and clinical PCV2 display two entirely opposing transcriptomic recalibrations of lymphoid tissue.

Introduction

Porcine circovirus type 2 (PCV2) manifests itself through a range of often devastating pathologies in swine livestock, causing severe economic losses. The most prominent disease associated with PCV2 is post-weaning multisystemic wasting syndrome (PMWS). PMWS patients exhibit progressive weight-loss, respiratory distress, pallor of skin, digestive disorders and sometimes jaundice, coinciding with pneumonia, nephritis, hepatitis and severe lymphadenopathy. Pathologic hallmarks in wasting pigs include progressive lymphocytic depletion and monocyte infiltration in lymph nodes [1], drastically compromising the immune system with often fatal outcome [2]. Although PCV2 is acknowledged as the causative agent of PMWS, PCV2 infection alone generally results in a persistent low-level replication without clinical signs [3]. In fact, PCV2 circulates endemically in pig populations as covert subclinical infections, seemingly undeterred by vaccination [4]. Pigs with PMWS however, are nearly always presented with concurrent microbial infections, suggesting a crucial role for superinfections in triggering PMWS [5]. Indeed, coinfections or other immunostimulations such

as adjuvant administration were confirmed to produce PMWS in experimental models [6]. Despite two decades of intensive research, real mechanistic insights into how PCV2 achieves subclinical persistence and why certain individuals transform from subclinical PCV2 to PMWS remain unknown.

Large data sets measuring the transcriptomic architecture of biological systems combined with new mathematical and statistical models are currently revolutionizing biomedical research. Major ongoing efforts focus on identifying and genetically perturbing regulatory networks at the core of pathological processes, to enable disease outcome prediction [7,8], phenotype classification [9,10] and drug discovery [11,12]. Specifically for the field of porcine biology, many individual data sets from live animals were analyzed within the study for which they were generated, and thus, integrated analysis of the recent wealth of transcriptomic data opens opportunities for systems biologists. Here we take advantage of large volumes of porcine transcriptomic studies to create a novel gene signature collection with hundreds of gene sets characterizing *in vivo* tissue perturbation, which we subsequently interrogated against circovirus patient studies to gain mechanistic insights into the pathogenesis of host responses to PCV2 viral infection.

Results

PorSignDB: a gene set collection characterizing a compendium of *in vivo* transcriptomic profiles

We first created PorSignDB, a collection of gene signatures, using a systematic approach previously developed for inference of the immunologic gene signature collection ImmuneSigDB [13]. Specifically, we compiled a large gene expression compendium curated from 88 studies including 1776 unique samples. A total of 412 annotated gene sets were derived from 206 pairwise comparisons identifying genes induced and repressed in one phenotype versus another, annotated as 'UP' (PHENOTYPE1_VS_PHENOTYPE2_UP) and

'DOWN' (PHENOTYPE1_VS_PHENOTYPE2_DN) gene sets, respectively (Fig 1A). To illustrate this, an example is given for a study comparing lymph nodes of uninfected pigs versus those of pigs experimentally infected with *Salmonella enterica Typhimurium* [14]. Upregulated genes (UP gene set) are highly expressed in the uninfected phenotype, while downregulated genes (DN gene set) are highly expressed in the *Salmonella*-infected phenotype (Fig 1B). Samples were predominantly derived from real-life patients or laboratory animals (1519 *in vivo* specimens and 236 *ex vivo* samples), and additionally include some from cell cultures (21 samples). The samples were derived from a multitude of different tissues (Fig 1C) and together, they describe host responses in an entire range of biological themes, with a major part stemming from studies on microbiology, gastroenterology and the cardiovascular system (Fig 1D).

Of note, porcine genes and individual probes were mapped to *Homo sapiens* ortholog genes. Because many transcriptional programs are evolutionarily conserved, cross-species gene expression analysis can be applied successfully [15,16]. Moreover, molecular signature databases are often human-oriented, and the porcine-to-human adaptation of PorSignDB thus facilitates its application to genomic expression data of any species. The PorSignDB gene signatures are available as an online resource (http://www.vetvirology.ugent.be/PorSignDB/) and can be used by systems biologists to deconvolute cellular circuitry in health and disease. As proof of concept, we employed this gene signature collection describing host responses in a wide variety of tissues to generate new insights in the multisystemic disease associated with PCV2.

PorSignDB reveals diametrically opposed physiological states *in vivo* in subclinical PCV2 and PMWS

We then leveraged PorSignDB to analyze a field study of pigs naturally affected with PMWS [17]. To compare transcriptomic profiles of PMWS lymph nodes with PCV2-positive but

126 otherwise healthy lymph nodes, we tested signatures from PorSignDB for their enrichment
127 (induced or repressed) in both classes using GSEA analysis (Fig 2A). We primarily focused
128 on gene sets pertaining to microbiology. For robustness, we only retained signatures from
129 pairwise comparisons in case both upregulated (PHENOTYPE1_VS_PHENOTYPE2_UP)
130 and downregulated (PHENOTYPE1_VS_PHENOTYPE2_DN) genes are significantly
131 enriched (FDR<0.01). For example, UP genes in splenic tissue of "control versus *Haemophilus*
132 *parasuis*-infected pigs" are suppressed (Fig 2B, left heatmap first row), while DN genes are
133 induced (Fig 2B, right heatmap first row).

134 Overall, this analysis reveals that upregulated genes in "control VS microbial challenge" are
135 suppressed while downregulated genes are induced. In other words, PMWS lymph nodes
136 display transcriptomic reprogramming consistent with tissue responses on infectious agents.
137 This observation is supported by previous findings that naturally occurring PMWS is presented
138 with concurrent infections [5]. Strikingly, two genomic infection signatures do not follow this
139 pattern. First, the opposite behavior of the gene signature from *Salmonella Typhimurium* 21
140 days post inoculation (dpi) suggests that the *Salmonella* infection has already been cleared at
141 this timepoint. This is indeed the case: at 21dpi the bacterial load in these mesenteric lymph
142 nodes was reduced to undetectable levels [18]. In contrast, *S. Choleraesuis* infection was
143 sustained at 21dpi, coinciding with persistent high bacterium abundance in mesenteric lymph
144 nodes. Intriguingly, the second deviating gene signature originates from pigs that were
145 subclinically infected with PCV2 (Fig 2A, arrow). Unlike *S. Typhimurium*, this cannot be
146 explained by pathogen clearance since these experimentally PCV2-infected pigs remained
147 viremic throughout the original study [19]. Instead, pathogen-distressed host responses
148 appear here to be repressed in lymph nodes with low-level subclinical PCV2 replication.
149 Hence, highly expressed genes in "uninfected VS subclinical PCV2-infected" lymph nodes are
150 induced, while lowly expressed genes are suppressed. From this data, it can be concluded
151 that subclinical PCV2 infection simulates pathogen-free tissue by reprogramming lymphoid
152 tissue diametrically opposite to an ongoing infection.

Finally, the gene sets PMWS_VS_HEALTHY_UP and PMWS_VS_HEALTHY_DN serve as positive control since they were derived from the data that was queried in this instance. PorSignDB signatures from other biological themes may provide additional clues into the alterations in lymph nodes that are subject to PMWS and could be explored further (Fig S1, see also discussion).

An immune response gene signature predicts clinical outcome of PCV2 disease

In an experimental setting, PCV2 alone does not lead to clinical signs. Additional superinfections or vaccination challenges are needed to produce PMWS [6]. Why extraneous immunostimulations trigger PMWS remains however poorly understood. A systems-level dissection of PCV2-affected lymphoid tissue may provide an explanation to this conundrum because it can determine which transcripts characterize PMWS, unbiased by previous knowledge. To this extent, the PMWS field study data was divided over a training and validation cohort, and 173 biomarker genes were selected from the training set using a leave-one-out cross validation (Fig 3A, Table S1). Together, they reveal a molecular portrait of PCV2-associated lymphoid lesions. This 'PCV2 disease signature' is greatly induced in the validation cohort as shown by GSEA analysis, meaning upregulation of PMWS marker genes and downregulation of Healthy marker genes (Fig 3B). Interestingly, in mediastinal lymph nodes with subclinical PCV2 at 29dpi, the disease signature is dramatically repressed when compared to lymph nodes of non-infected counterparts, showing once more that subclinical PCV2 actively suppresses the transcriptomic recalibration that goes hand in hand with PMWS. To illustrate the fidelity of the PCV2 disease signature, individual samples were classified as either PMWS or healthy with the Nearest Template Prediction algorithm [20]. All samples of the validation set were correctly assigned (FDR <0.05; Fig 3C). Furthermore, all piglets from the experimental study, either PCV2 free or with subclinical PCV2, were correctly classified as Healthy with only one sample failing to meet the <0.05 FDR threshold (Fig 3D). Furthermore, when performing a Gene Ontology overrepresentation test, the PMWS

biomarker genes clearly represent the immune response, which confirms from a systems level that immune activation is a pivotal event in PMWS (Fig S2A). Of note, this gene signature performs better than an RNMI-based signature (Fig S2B-C), which is more suited for small sample sizes and was therefore applied for generating PorSignDB.

Interestingly, when probing the kinetics of the PCV2 disease signature in lymph nodes of pigs experimentally infected with PCV2, *S. Typhimurium* or *S. Choleraesuis*, it is clear that these two bacterial infections promote the disease signature, while in subclinical PCV2 it is consistently suppressed (Fig 3E-G). In *S. Typhimurium* the reversal of this clinical gene signature at 21 dpi coincides with the drop of bacterial load in the mesenteric lymph nodes to almost undetectable degree. This demonstrates from a systems-approach that the infection has been virtually cleared at this time point, unlike mesenteric lymph nodes upon *S. Choleraesuis* infection, where the persistence of the signature correlates with an enduring high bacterial lymph node colonization [18].

Taken together, PCV2-induced lymphoid depletion and granulomatous inflammation in PMWS patients can be summarized in a robust gene expression signature emblematic of an enduring immune activation. Moreover, through an impartial systems-approach, we irrefutably show that a subclinical PCV2 inoculation provokes a striking suppression of the immune response.

Functional genomics identify regulatory networks perturbations in PCV2 disease

It is becoming increasingly clear that PMWS and subclinical PCV2 represent two opposing adaptations of lymphoid tissue to circoviral infection. The former enhances immune system activation and fulminant viremia, whereas in the latter the immune system stays deafeningly silent with only a mild viremia. To understand how this tiny virus arranges this *tour de force*, the data sets covering both the PMWS field study [17] and the experimentally induced subclinical PCV2 at 29 dpi [19] were interrogated in the GSEA computational system with the

innovative Hallmark gene set collection [21]. This provides a very sensitive overview of alterations in a number of key regulatory networks and signaling pathways in both PMWS patients (Fig 4, left column) and pigs with persistent subclinical PCV2 (Fig 4A, right column). In lymphoid tissue of pigs with PMWS, many of the affected transcriptional networks echo key events in PCV2-associated lymphopathology such as blatant inflammatory activity (Hallmark gene set 'Inflammatory response') and caspase-mediated cell death ('Apoptosis'). Increases in gene expression mediated by p53 ('p53 pathways), reactive oxygen species ('ROS pathway') and NF-κB ('TNFα signaling through NFκB') reflect findings that PCV2 promotes p53 expression [22,23] and triggers NFκB activation through ROS [24,25] (Fig 4, left column). This analysis not only indicates critical adjustments for amplified viral replication, it also uncovers several previously unknown network modifications. These include immunological programs ('Interferon alpha response' and 'Interferon gamma response'), cell signaling cascades ('IL2-STAT5 signaling', 'IL6-JAK-STAT3 signaling', 'KRAS signaling up') and bioenergetics ('Glycolysis' and 'Hypoxia').

Consistent with previous results, subclinical PCV2 infection generally fails to reproduce the imbalances associated with PMWS (Fig 4, right column). Only the transcriptomic programs downstream of interferon-α and interferon-γ are in line with subclinical infections, suggesting a direct viral effect on these immunological networks. Most programs are however unaffected or opposed to the changes occurring in PMWS, reaffirming the running thread that subclinical PCV2 is unable to reprogram the circuitry to develop PMWS.

IL-2 supplementation enables *ex vivo* modelling of PCV2 in primary porcine lymphoblasts

The transcriptional upregulation of IL-2 responsive genes in PMWS, but not in subclinical PCV2 (Fig 4A), indicates that fulminant PCV2 replication occurs in an IL-2 infused lymphoid environment. Given the pivotal role of IL-2 in activated T-cells during immune response [26],

IL-2 may indeed be a crucial factor in boosting subclinical PCV2 towards PMWS. Intriguingly, the IL2-STAT5 signaling network is suppressed in subclinical PCV2, but not in *S. Choleraesuis* and *S. Typhimurium*, where there is a persistent and transient induction respectively (Fig 5A). Again, in *S. Typhimurium*, the reversal of the IL-2 signature coincides with bacterial clearance.

The impact of IL-2 on PCV2 replication cannot be faithfully demonstrated with traditional PK15 kidney cells. Because PCV2 has a tropism for lymphoblasts, these are the cells of choice. Our lab previously demonstrated that treatment of freshly harvested PBMCs with concanavalin A (ConA) coerces T-cells into mitosis, rendering them permissive for PCV2 [27]. Unfortunately, lymphoblast proliferation can only be maintained for a very short time after which the cells forfeit viability and die of attrition. Indeed, when isolated lymphocytes are stimulated with ConA without IL-2, these cells start suffering from apoptosis even before the first passage at 72h. However, supplementing ConA-stimulated lymphocytes with IL-2 not only mimics the PMWS microenvironment, it generates continuously expanding primary porcine lymphoblasts (PPLs; Fig 5B-C). These PPLs can be easily cultured, expanded and infected with PCV2 *ex vivo*, providing a cell culture platform amenable for studying PMWS pathogenesis (Fig 5D). To prove the beneficial effect of IL-2 on PCV2 replication, lymphocytes were freshly harvested from six individual pigs. IL-2 supplementation doubled PCV2 infection rates after 36h, a timeframe amounting to a single round of replication (Fig 5E). This demonstrates that T-cell activation by IL-2 fosters PCV2 infection and highlights the potential of PPLs for studying PMWS.

STAT3 is a PCV2 host factor and a target for antiviral intervention

Since transcriptional networks of PMWS lymphoid tissue are subject to dramatic changes that correlate with fulminant PCV2 replication, counteracting these alterations can potentially harm the viral life cycle. When observing a fierce induction of gene expression downstream the IL6-JAK-STAT3 signaling cascade in PCV2 patients (Fig S2A), STAT3 emerges as a druggable

candidate host factor. Interestingly, STAT3 is a key regulator of inflammation often exploited by viruses with pathogenic consequences [28]. In a drug assay, treatment with selective STAT3 inhibitor Cpd188 exhibits a dose-dependent effect on PCV2 infection in PPLs at 72 hpi (Fig 6A). Cell viability assay reveals no toxicity, excluding non-specific adverse effects of the compound on infection (Fig 6B). Chemical inhibition also displays a dose-dependent effect on PCV2 infection in PK15 cells (Fig S2B-D). Thus, robust expression of STAT3 responsive genes are critical for PCV2, and hampering STAT3 activity represents an antiviral strategy (Fig 6C).

A paracrine macrophage-lymphoblast communication axis exacerbates PCV2 infection

Finally, the PMWS field study dataset was queried in GSEA with ImmuneSigDB's immunological gene signatures [13]. This revealed a striking suppression of lymphocyte gene expression and powerful induction of signatures from monocytes and other myeloid cells (Fig 7A, Table S2), reflecting the loss of lymphocytes and histiocytic replacement in PMWS lymph nodes. This raises the question to what extent infiltrating monocytes affect PCV2 replication. After maturation into macrophages, they may either dampen infection by destroying viral particles, or promote PCV2 in a paracrine fashion by releasing pro-inflammatory cytokines. To test the effect of intercellular communication between macrophages and lymphocytes, a co-culture experiment was set up. PCV2-infected PPLs were seeded in a porous insert, physically separated from a lower compartment with primary porcine macrophages (Fig 7B). The latter were challenged with Porcine Reproductive and Respiratory Syndrome Virus (PRRSV), a virus that can experimentally trigger PMWS [6] (Fig 7C). The presence of non-infected macrophages had no significant effect on PCV2 lymphoblast infection levels, but when co-cultured with PRRSV-infected macrophages, a significant and consistent increase in PCV2 infection could be discerned (Fig 7D). This demonstrates the existence of a previously

284 unknown axis of intercellular communication between macrophages and lymphoblasts
285 exacerbating PCV2 replication.

286

287 ## Discussion

288 Systems biology approaches aim to model regulatory networks from genome-wide
289 transcriptional profiles as a large interconnected switchboard where many small inputs
290 combine to execute large programs. In response to extra- or intracellular stimuli, cells will
291 modify their circuitry in an orchestrated effort to adapt to their environment. These days,
292 mapping genome-wide transcripts for biological network analysis has become fast, cheap and
293 easy. Especially when deposited in public databases, it provides an ever-growing library of
294 transcriptomes. Here we unlock the potential of porcine microarray studies by turning it into
295 an atlas of tissue transcripts for bioinformatical analysis, extending the MSigDB database with
296 *in vivo* derived profiles [29]. Prior mapping of porcine microarray probes to human orthologs
297 facilitates its application to any mammalian gene expression data set.

298 PorSignDB is especially convenient for delineating which physiological state one's samples of
299 interest resemble, generating useful hypotheses in the process. When applied to PCV2 patient
300 data, it elegantly exposes the transcriptomic bedrock underlying circoviral persistence: PCV2
301 reprograms lymph node circuitry into a state of non-infection as a strategy for establishing
302 covert chronic infection. We hereby postulate the mechanics of how PCV2 operates in swine
303 livestock. In an initial phase, PCV2 functionally silences the immune response, delaying or
304 even completely abrogating an adaptive antibody response [30]. This recalibration allows only
305 low-level PCV2 replication but does result in viral persistence without clinical signs. Only when
306 PCV2's input on host transcriptomics is overturned by a severe superinfection are
307 inflammatory networks and STAT3 responsive gene expression engaged. This immune
308 activation infuses lymphoid tissue with IL-2 to activate T-cells into lymphoblasts, triggering
309 fulminant circoviral replication and widespread lymphocyte apoptosis. When macrophages

rush in to help, their paracrine signaling exacerbates PCV2 replication even further. Moreover, PCV2 capsids resist destruction by macrophages, which fuse together into histiocytic giant cells in an ineffective last-ditch effort to stem the infection. PMWS is thus the end-stage of a lethal viral lymph node disease, where germinal centers have collapsed and functional parenchyma is replaced by macrophages, leading to a structural immune deficiency.

Confronted with the evidence that subclinical PCV2 and PMWS are two different host reactions to PCV2, we deem it important to discriminate between these two phenotypes of 'PCV2 infection'. Treating them as a single entity will only result in conflicting data. As an example, this integrative transcriptional analysis resolves the long-standing dichotomy in PMWS pathology of whether or not apoptosis is implicated in lymphoid depletion *in vivo* [31–33]. In lymphoid tissue with low-level replication, it is not. On the other hand, in lymph nodes collapsing under PCV2, genes mediating apoptosis are in full force (Fig 4).

Another example of PorSignDB generating intriguing hypotheses, is that weaned gut gene expression signatures are induced in clinical PCV2, while intestinal signatures of suckling piglets are suppressed (Fig S1). It suggests that as long as intestinal tissue is protected by maternal antibodies, progression to PMWS is obstructed. On the other hand, when weaned, naive intestinal tissue makes immunological contact with pathogens, producing a microenvironment that reflects PMWS and hence, can promote PCV2.

Finally, the pronounced IL-2 signature in clinical PCV2 inspired the establishment of primary lymphoblast strains. They can be easily expanded and stored in liquid nitrogen, and display excellent post-thaw survival. Unlike PK-15 cells, they can be harvested from different individuals or breeds, providing a new and valuable tool for studying the long-suspected impact of genetic background on PCV2 disease [34,35].

In conclusion, we here solve a long-standing enigma of how PCV2 establishes subclinical persistence, and how it switches to clinical disease. Upon infection, host tissue is instructed to act as if the pathogen is absent, allowing PCV2 to replicate covertly at modest rates.

Whenever an individual falls victim to a stimulus that rewires the transcriptional circuitry into immune activation, PCV2 replicates frantically and overwhelms the host. Given its limited coding capacity, PCV2 cannot manage it alone but depends on superinfections to recalibrate the host. This elegantly explains how PCV2 circulates in pig farms, and settles the controversies that have haunted PCV2 pathologists.

Materials and methods

Generating PorSignDB

Raw Affymetrix Porcine Genechip data were retrieved from NCBI GEO (http://www.ncbi.nlm.nih.gov/geo/). Data covering pooled samples or lacking publication on Pubmed were discarded, as were studies with <2 samples per phenotype. Quantile normalized expression data was generated from .CEL files using the ExpressionFileCreator module on Genepattern [36]. Affymetrix probe set identifiers were mapped to Homo sapiens gene symbols as previously described [37] with Refseq and Uniprot identifiers were changed into corresponding gene symbols. Early transcriptional responses (<30 mins) and comparisons between breeds or tissue types were ignored. If controls were unavailable for temporal studies, comparisons were made with t=0. For signature generation, the ImmuneSigDB recipe [13] was followed. Briefly, genes were correlated to a target profile and ranked using the RNMI metric [38]. Top and bottom ranked genes with an FDR <0.01 in a permutation test were included in two gene sets, with maximally 200 genes each, yielding PHENOTYPE1_VS_PHENOTYPE2_UP" and "PHENOTYPE1_VS_PHENOTYPE2_DN".

PCV2 disease signature and phenotype classification

Biomarker genes were calculated from data of a field study covering three different cohorts [17], according to a previously described method [7] with minor modifications. Cohorts were divided over a training set (n=17) and a validation set (n=8). Marker genes were ranked in the

362 training set using signal-to-noise ratio (S2NR), with standard deviations adjusted to minimally
363 0.2*mean. In a subsequent leave-one-out cross validation, a single sample was left out and a
364 permutation test was performed on the remaining samples. Only genes with $p<0.05$ in every
365 iterative leave-one-out trial were included in the signature. For phenotype classification, the
366 NTP algorithm [20] was employed with S2NR as weights.
367

368 **Cells, virus and reagents**

369 PK15 kidney cells were a kind gift of Gordon Allan, Queen's University, Belfast, UK. PK15
370 culture conditions were described earlier [39]. To generate PPLs, PBMCs were isolated as
371 described previously (Lefebvre *et al.*, 2008b). After adhering of monocytes to a plastic culture
372 flask, lymphocytes in suspension were pelleted, resuspended in culture medium
373 supplemented with 5 µg/ml ConA (Sigma) and 50 µM β-mercaptoethanol (Gibco). After three
374 days, cells were pelleted, washed with RPMI (Gibco), and resuspended in culture medium
375 supplemented with 100 U/ml human recombinant IL-2 (NIH) and 50 µM β-mercaptoethanol.
376 Porcine alveolar macrophages were isolated as described [40]. Animal procedures were
377 approved by Ghent University ethical committee EC2013/97. PCV2 strains 1121 and
378 Stoon1010 were described previously [41]. PRRSV Lelystad strain was described earlier [40].
379 Cpd188 was ordered from Merck Millipore.
380

381 **Experimental infection and immunostaining**

382 PK-15 and PPLs were inoculated with PCV2 1121 at 0.1 $TCID_{50}$/cell for 1h, washed and further
383 incubated in culture medium for 36h. For Cpd188 experiments, cells were pre-incubated for
384 1 hour with Cpd188 (Merck Millipore) dissolved in 0.25 % DMSO. Subsequently, cells were
385 inoculated with PCV2 at 0.1 $TCID_{50}$/cell for 1h, washed and incubated for 72h. For co-culture,
386 PPLs and macrophages were inoculated at 0.5 $TCID_{50}$/cell for 1h with PCV2 Stoon1010 and

PRRSV respectively, washed and incubated for 72h. PCV2 capsid immunostaining with mAb 38C1 was described earlier (Huang *et al.*, 2015).

Acknowledgements

We thank Joaquím Segalés and Lana T. Fernandes for sharing clinical data, Hussein El-Saghire, Gerben Menschaert and Eloi E.R. Verrier for helpful discussions, and Carine Boone for technical assistance.

References

1. Segalés J. Porcine circovirus type 2 (PCV2) infections: clinical signs, pathology and laboratory diagnosis. Virus Res. 2012;164: 10–19. doi:10.1016/j.virusres.2011.10.007

2. Darwich L, Mateu E. Immunology of porcine circovirus type 2 (PCV2). Virus Res. 2012;164: 61–67. doi:10.1016/j.virusres.2011.12.003

3. Opriessnig T, Prickett JR, Madson DM, Shen H-G, Juhan NM, Pogranichniy RR, et al. Porcine circovirus type 2 (PCV2)-infection and re-inoculation with homologous or heterologous strains: virological, serological, pathological and clinical effects in growing pigs. Vet Res. 2010;41: 31. doi:10.1051/vetres/2010003

4. Xiao C-T, Harmon KM, Halbur PG, Opriessnig T. PCV2d-2 is the predominant type of PCV2 DNA in pig samples collected in the U.S. during 2014-2016. Vet Microbiol. 2016;197: 72–77. doi:10.1016/j.vetmic.2016.11.009

5. Opriessnig T, Halbur PG. Concurrent infections are important for expression of porcine circovirus associated disease. Virus Res. 2012;164: 20–32. doi:10.1016/j.virusres.2011.09.014

6. Tomás A, Fernandes LT, Valero O, Segalés J. A meta-analysis on experimental infections with porcine circovirus type 2 (PCV2). Vet Microbiol. 2008;132: 260–273. doi:10.1016/j.vetmic.2008.05.023

7. Hoshida Y, Villanueva A, Kobayashi M, Peix J, Chiang DY, Camargo A, et al. Gene expression in fixed tissues and outcome in hepatocellular carcinoma. N Engl J Med. 2008;359: 1995–2004. doi:10.1056/NEJMoa0804525

8. van de Vijver MJ, He YD, van't Veer LJ, Dai H, Hart AAM, Voskuil DW, et al. A gene-expression signature as a predictor of survival in breast cancer. N Engl J Med. 2002;347: 1999–2009. doi:10.1056/NEJMoa021967

9. Golub TR, Slonim DK, Tamayo P, Huard C, Gaasenbeek M, Mesirov JP, et al. Molecular classification of cancer: class discovery and class prediction by gene expression monitoring. Science. 1999;286: 531–537.

10. Hoshida Y, Nijman SMB, Kobayashi M, Chan JA, Brunet J-P, Chiang DY, et al. Integrative transcriptome analysis reveals common molecular subclasses of human hepatocellular carcinoma. Cancer Res. 2009;69: 7385–7392. doi:10.1158/0008-5472.CAN-09-1089

11. Lamb J, Crawford ED, Peck D, Modell JW, Blat IC, Wrobel MJ, et al. The Connectivity Map: using gene-expression signatures to connect small molecules, genes, and disease. Science. 2006;313: 1929–1935. doi:10.1126/science.1132939

12. Subramanian A, Narayan R, Corsello SM, Peck DD, Natoli TE, Lu X, et al. A Next Generation Connectivity Map: L1000 Platform and the First 1,000,000 Profiles. Cell. 2017;171: 1437-1452.e17. doi:10.1016/j.cell.2017.10.049

13. Godec J, Tan Y, Liberzon A, Tamayo P, Bhattacharya S, Butte AJ, et al. Compendium of Immune Signatures Identifies Conserved and Species-Specific Biology in Response to Inflammation. Immunity. 2016;44: 194–206. doi:10.1016/j.immuni.2015.12.006

14. Wang Y, Couture OP, Qu L, Uthe JJ, Bearson SMD, Kuhar D, et al. Analysis of porcine transcriptional response to Salmonella enterica serovar Choleraesuis suggests novel targets of NFkappaB are activated in the mesenteric lymph node. BMC Genomics. 2008;9: 437. doi:10.1186/1471-2164-9-437

15. Lu Y, Huggins P, Bar-Joseph Z. Cross species analysis of microarray expression data. Bioinformatics. 2009;25: 1476–1483. doi:10.1093/bioinformatics/btp247

16. Kristiansson E, Österlund T, Gunnarsson L, Arne G, Larsson DGJ, Nerman O. A novel method for cross-species gene expression analysis. BMC Bioinformatics. 2013;14: 70. doi:10.1186/1471-2105-14-70

17. Fernandes LT, Tomás A, Bensaid A, Sibila M, Sánchez A, Segalés J. Microarray analysis of mediastinal lymph node of pigs naturally affected by postweaning multisystemic wasting syndrome. Virus Res. 2012;165: 134–142. doi:10.1016/j.virusres.2012.02.006

18. Uthe JJ, Royaee A, Lunney JK, Stabel TJ, Zhao S-H, Tuggle CK, et al. Porcine differential gene expression in response to Salmonella enterica serovars Choleraesuis and Typhimurium. Mol Immunol. 2007;44: 2900–2914. doi:10.1016/j.molimm.2007.01.016

19. Tomás A, Fernandes LT, Sánchez A, Segalés J. Time course differential gene expression in response to porcine circovirus type 2 subclinical infection. Vet Res. 2010;41: 12. doi:10.1051/vetres/2009060

20. Hoshida Y. Nearest template prediction: a single-sample-based flexible class prediction with confidence assessment. PLoS ONE. 2010;5: e15543. doi:10.1371/journal.pone.0015543

21. Liberzon A, Birger C, Thorvaldsdóttir H, Ghandi M, Mesirov JP, Tamayo P. The Molecular Signatures Database (MSigDB) hallmark gene set collection. Cell Syst. 2015;1: 417–425. doi:10.1016/j.cels.2015.12.004

22. Karuppannan AK, Liu S, Jia Q, Selvaraj M, Kwang J. Porcine circovirus type 2 ORF3 protein competes with p53 in binding to Pirh2 and mediates the deregulation of p53 homeostasis. Virology. 2010;398: 1–11. doi:10.1016/j.virol.2009.11.028

23. Liu J, Zhu Y, Chen I, Lau J, He F, Lau A, et al. The ORF3 protein of porcine circovirus type 2 interacts with porcine ubiquitin E3 ligase Pirh2 and facilitates p53 expression in viral infection. J Virol. 2007;81: 9560–9567. doi:10.1128/JVI.00681-07

24. Chen X, Ren F, Hesketh J, Shi X, Li J, Gan F, et al. Reactive oxygen species regulate the replication of porcine circovirus type 2 via NF-κB pathway. Virology. 2012;426: 66–72. doi:10.1016/j.virol.2012.01.023

25. Wei L, Kwang J, Wang J, Shi L, Yang B, Li Y, et al. Porcine circovirus type 2 induces the activation of nuclear factor kappa B by IkappaBalpha degradation. Virology. 2008;378: 177–184. doi:10.1016/j.virol.2008.05.013

26. Boyman O, Sprent J. The role of interleukin-2 during homeostasis and activation of the immune system. Nat Rev Immunol. 2012;12: 180–190. doi:10.1038/nri3156

27. Lefebvre DJ, Meerts P, Costers S, Misinzo G, Barbé F, Van Reeth K, et al. Increased porcine circovirus type 2 replication in porcine leukocytes in vitro and in vivo by concanavalin A stimulation. Vet Microbiol. 2008;132: 74–86. doi:10.1016/j.vetmic.2008.05.004

28. Roca Suarez AA, Van Renne N, Baumert TF, Lupberger J. Viral manipulation of STAT3: Evade, exploit, and injure. PLoS Pathog. 2018;14: e1006839. doi:10.1371/journal.ppat.1006839

29. Liberzon A, Subramanian A, Pinchback R, Thorvaldsdóttir H, Tamayo P, Mesirov JP. Molecular signatures database (MSigDB) 3.0. Bioinformatics. 2011;27: 1739–1740. doi:10.1093/bioinformatics/btr260

30. Opriessnig T, Gerber PF, Matzinger SR, Meng X-J, Halbur PG. Markedly different immune responses and virus kinetics in littermates infected with porcine circovirus type 2 or porcine parvovirus type 1. Vet Immunol Immunopathol. 2017;191: 51–59. doi:10.1016/j.vetimm.2017.08.003

31. Lin C-M, Jeng C-R, Hsiao S-H, Liu J-P, Chang C-C, Chiou M-T, et al. Immunopathological characterization of porcine circovirus type 2 infection-associated follicular changes in inguinal lymph nodes using high-throughput tissue microarray. Vet Microbiol. 2011;149: 72–84. doi:10.1016/j.vetmic.2010.10.018

32. Resendes AR, Majó N, Segalés J, Mateu E, Calsamiglia M, Domingo M. Apoptosis in lymphoid organs of pigs naturally infected by porcine circovirus type 2. J Gen Virol. 2004;85: 2837–2844. doi:10.1099/vir.0.80221-0

33. Shibahara T, Sato K, Ishikawa Y, Kadota K. Porcine circovirus induces B lymphocyte depletion in pigs with wasting disease syndrome. J Vet Med Sci. 2000;62: 1125–1131.

34. Opriessnig T, Fenaux M, Thomas P, Hoogland MJ, Rothschild MF, Meng XJ, et al. Evidence of breed-dependent differences in susceptibility to porcine circovirus type-2-associated disease and lesions. Vet Pathol. 2006;43: 281–293. doi:10.1354/vp.43-3-281

35. Opriessnig T, Patterson AR, Madson DM, Pal N, Rothschild M, Kuhar D, et al. Difference in severity of porcine circovirus type two-induced pathological lesions between Landrace and Pietrain pigs. J Anim Sci. 2009;87: 1582–1590. doi:10.2527/jas.2008-1390

36. Reich M, Liefeld T, Gould J, Lerner J, Tamayo P, Mesirov JP. GenePattern 2.0. Nat Genet. 2006;38: 500–501. doi:10.1038/ng0506-500

37. Tsai S, Cassady JP, Freking BA, Nonneman DJ, Rohrer GA, Piedrahita JA. Annotation of the Affymetrix porcine genome microarray. Anim Genet. 2006;37: 423–424. doi:10.1111/j.1365-2052.2006.01460.x

38. Cowley GS, Weir BA, Vazquez F, Tamayo P, Scott JA, Rusin S, et al. Parallel genome-scale loss of function screens in 216 cancer cell lines for the identification of context-specific genetic dependencies. Sci Data. 2014;1: 140035. doi:10.1038/sdata.2014.35

39. Huang L, Van Renne N, Liu C, Nauwynck HJ. A sequence of basic residues in the porcine circovirus type 2 capsid protein is crucial for its co-expression and co-localization with the replication protein. J Gen Virol. 2015;96: 3566–3576. doi:10.1099/jgv.0.000302

40. Labarque GG, Nauwynck HJ, Van Reeth K, Pensaert MB. Effect of cellular changes and onset of humoral immunity on the replication of porcine reproductive and respiratory syndrome virus in the lungs of pigs. J Gen Virol. 2000;81: 1327–1334. doi:10.1099/0022-1317-81-5-1327

41. Lefebvre DJ, Costers S, Van Doorsselaere J, Misinzo G, Delputte PL, Nauwynck HJ. Antigenic differences among porcine circovirus type 2 strains, as demonstrated by the use of monoclonal antibodies. J Gen Virol. 2008;89: 177–187. doi:10.1099/vir.0.83280-0

Supporting Information Legends

Figure S1 PorSignDB performance in lymph nodes of PMWS pigs VS healthy pigs. Figure displays enriched PorSignDB gene sets in the PMWS study pertaining to biological themes other than microbiology.

Figure S2 PMWS biomarker genes annotation and performance of an alternative clinical disease signature. **A** Gene ontology (GO) terms overrepresentation test of PMWS biomarker genes. **B** Nearest Template Prediction of test set samples using an alternative clincal gene signature based on the RNMI metric **C** and similarly, of the experimental subclinical infection samples at 29dpi.

Figure S3 STAT3 is a host factor in PCV2 disease. **A** Core genes responsible for the STAT3 signature enrichment score. **B** STAT3-specific inhibitor cpd-188 impairs infection in PK-15 cells. Means ± sd represents three independent experiments in triplicate (n=9; **P<0.01, ***P<0.001, Mann-Whitney U-Test). **C** MTT cell viability assay of cpd-188 treatment in PK-15 cells. Means ± sd are shown for three independent experiments in quintuplicate (n=15). **D** Infection assessment by PCV2 capsid immunostaining, representative figures for each treatment. Scale bar: 100 µm.

Table S1 Complete list of PCV2 disease signature biomarker genes.

Table S2 ImmuneSigDB analysis of the PMWS field study dataset.

Figure legends

Figure 1 Details of PorSignDB. **A** Overview of the pipeline. 88 curated studies with data from 1776 microarrays chips were retrieved from the GEO repository. Data from each study was uniformly normalized using Genepattern, and gene expression signatures representing each phenotype of every pairwise comparison were calculated in R. Systematical annotations were added to every signature, yielding 412 gene sets. **B** Example of signature generation. GSE7313 is a study mapping transcript abundance in mesenteric lymph nodes of pigs infected with *Salmonella Typhimurium* at different time points. The first pair compares data from lymph nodes of uninfected pigs (Phenotype1) with those of pigs 8h post *S. Typhimurium* infection (Phenotype2). Significantly upregulated and downregulated genes were selected with a mutual-information based metric, respectively recapitulating highly expressed genes in the 'uninfected' phenotype (UP gene set), and highly expressed genes in the '8h post *S.*

562 *Typhimurium* infection' phenotype (DN gene set). **C** Samples were derived from a variety of
563 different tissues, **D** covering studies in a wide range of different biological themes.

564 **Figure 2** Application of PorSignDB to lymph node data originating from pig farms with naturally
565 occurring PMWS. **A** Outline of the analysis. Data from PMWS-affected farms were retrieved
566 from GEO. In PMWS lymph nodes, follicular structures become indistinct and B-cells and T-
567 cells all but disappear, while infiltrating macrophages fuse into multi-nucleated giant cells. In
568 PCV2-positive healthy lymph nodes, lymphoid structure is intact. Comparing transcriptomes
569 of both phenotypes using GSEA displays enrichment of PorSignDB transcriptional signatures.
570 **B** Microbiology-related PorSignDB gene set expression in lymph nodes of PMWS pigs versus
571 Healthy pigs (FDR<0.01 and opposite expression of each pairwise phenotype). The average
572 expression of the leading-edge genes in every gene set (genes that contribute to the
573 enrichment) are displayed for each patient sample. Bars next to each gene set indicate the
574 signed FDR for its enrichment in log10 scale.

575 **Figure 3** A patient-derived immune response signature predicts clinical outcome of PCV2
576 infection. **A** Diagram of cohort division between training and test set. A clinical PCV2 signature
577 was calculated from the training samples and **B** tested in the validation samples by GSEA.
578 The PCV2 disease signature was markedly induced in the validation set, and repressed in
579 subclinical PCV2 29dpi. **C** Nearest Template Prediction of test set samples, classifying them
580 either as healthy (blue) or PMWS (red), and **D** similarly, of the experimental subclinical
581 infection samples at 29dpi. **E-G** Kinetics of the PCV2 disease signature upon experimental
582 PCV2, *S. Typhimurium* and *S. Choleraesuis* infection.

583 **Figure 4** Functional genetic networks of the Hallmark gene set collection that are markedly
584 altered in lymph nodes of pigs with PCV2. Left column: expression level in lymph nodes of
585 PMWS patients (FDR<0.01). Right column: expression-level of these biological circuits in
586 Subclinical PCV2 at 29dpi.

587 **Figure 5** IL-2 is implicated in PCV2 disease. **A** Kinetics of IL-2 responsive gene expression
588 (Hallmark IL2-STAT5 SIGNALING) upon three microbial infections: PCV2 (blue), *S.*
589 *Typhimurium* (orange) and *S. Choleraesuis* (green). **B** IL-2 activation of freshly isolated and
590 ConA-stimulated lymphocytes maintains exponential cellular proliferation, yielding primary
591 porcine lymphoblast (PPL) cell strains. Means ± sd represent one experiment in triplicate
592 (n=3). **C** Representative image of proliferating PLLs. Scale bar: 50 µm. **D** PCV2 Cap
593 immunostaining in PLLs 36hpi. Scale bar: 100 µm. **E** IL-2 supplementation doubles PCV2
594 infection after a single round of replication (36 hpi). Dot blot shows six single independent
595 experiments with horizontal line indicating median value (n=6; **P<0.01, two-tailed Mann-
596 Whitney). PPL cell strains were generated from six different individuals.

597 **Figure 6** STAT3 is a PCV2 host factor. **A** STAT3-specific inhibitor Cpd188 impairs infection
598 in PPLs. Means ± sd represent three independent experiments in triplicate (n=9; *P<0.05,
599 **P<0.01, two-tailed Mann-Whitney). **B** MTT lymphoblast viability assay of Cpd188 treatment.
600 Means ± sd are shown for three experiments in quintuplicate (n=15). **C** Cartoon outlining
601 STAT3 as a drugable host factor for PCV2 in lymphoblasts.

602 **Figure 7** Superinfection increases PCV2 replication through a macrophage-lymphoblast
603 paracrine signaling axis. **A** ImmuneSigDB gene set expression in the PMWS field study
604 (FDR<0.01 and opposite expression of each pairwise phenotype). The average expression of
605 the leading-edge genes in every gene set (genes that contribute to the enrichment) are
606 displayed for each patient sample. Bars next to each gene set indicate the signed FDR for its
607 enrichment in log10 scale. PMWS versus healthy lymph node comparison displays a dramatic
608 repression of lymphocyte gene expression signatures, and induction of myeloid cell
609 signatures. **B** Experimental set-up of PPL-macrophage co-culture system mimicking PMWS
610 lymph nodes. **C** PCV2-inoculated PPLs were seeded on a porous insert with macrophages at
611 the bottom of the well. Macrophages were additionally challenged with PRRSV at 0h. **D**
612 Relative PPL infection levels at 72hpi. Means ± sd represent two independent experiments in
613 triplicate (n=6; *P<0.05, two-tailed Mann-Whitney).

614

Figure 1

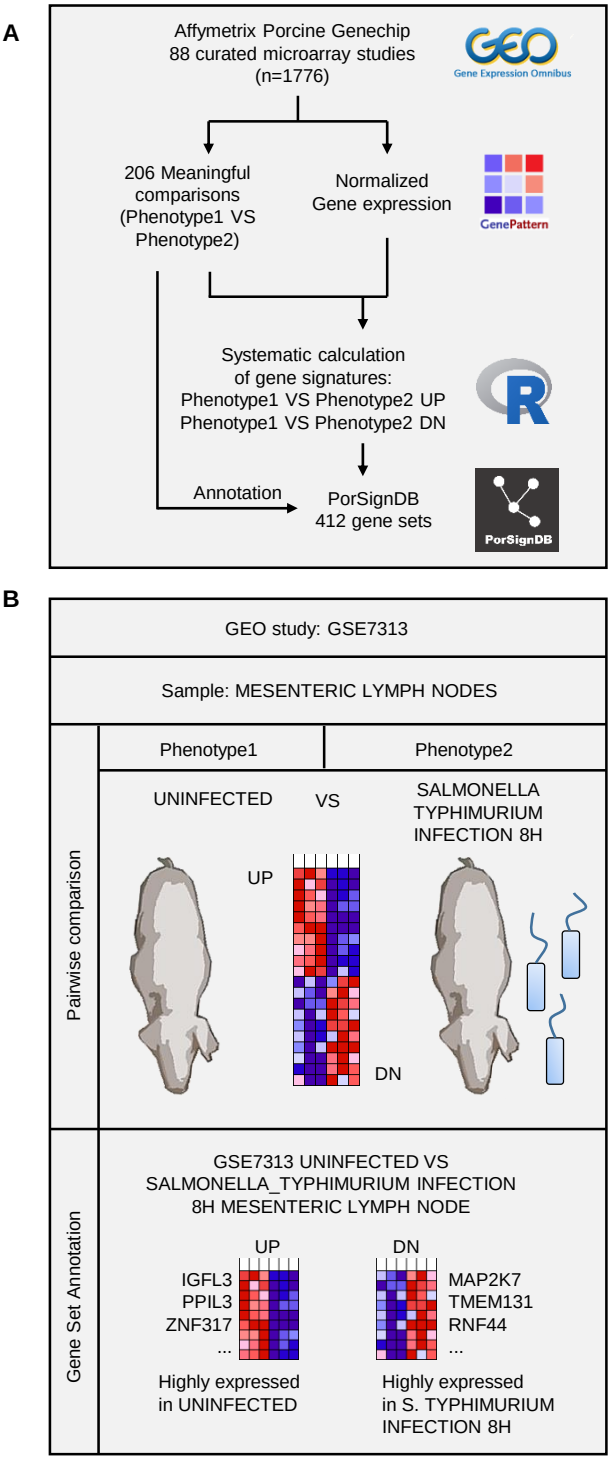
A
Affymetrix Porcine Genechip
88 curated microarray studies
(n=1776)
Gene Expression Omnibus
206 Meaningful
comparisons
(Phenotype1 VS
Phenotype2)
Normalized
Gene expression
GenePattern
Systematic calculation
of gene signatures:
Phenotype1 VS Phenotype2 UP
Phenotype1 VS Phenotype2 DN
Annotation
PorSignDB
412 gene sets
PorSignDB
B
GEO study: GSE7313
Sample: MESENTERIC LYMPH NODES
Phenotype1
Phenotype2
UNINFECTED
VS
SALMONELLA
TYPHIMURIUM
INFECTION 8H
UP
DN
Pairwise comparison
Gene Set Annotation
GSE7313 UNINFECTED VS
SALMONELLA_TYPHIMURIUM INFECTION
8H MESENTERIC LYMPH NODE
UP
DN
IGFL3
PPIL3
ZNF317
...
MAP2K7
TMEM131
RNF44
...
Highly expressed
in UNINFECTED
Highly expressed
in S. TYPHIMURIUM
INFECTION 8H

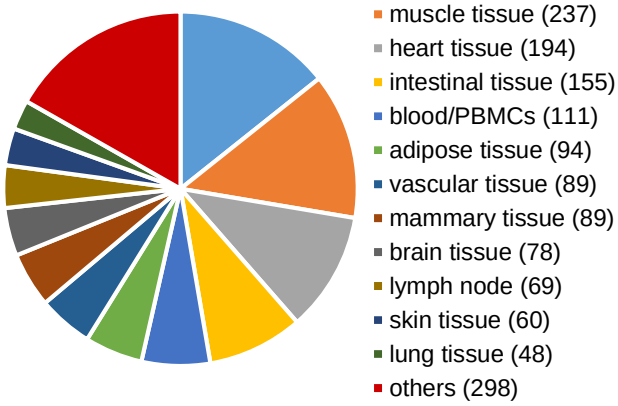
C
Origin of samples
liver tissue (254)
muscle tissue (237)
heart tissue (194)
intestinal tissue (155)
blood/PBMCs (111)
adipose tissue (94)
vascular tissue (89)
mammary tissue (89)
brain tissue (78)
lymph node (69)
skin tissue (60)
lung tissue (48)
others (298)

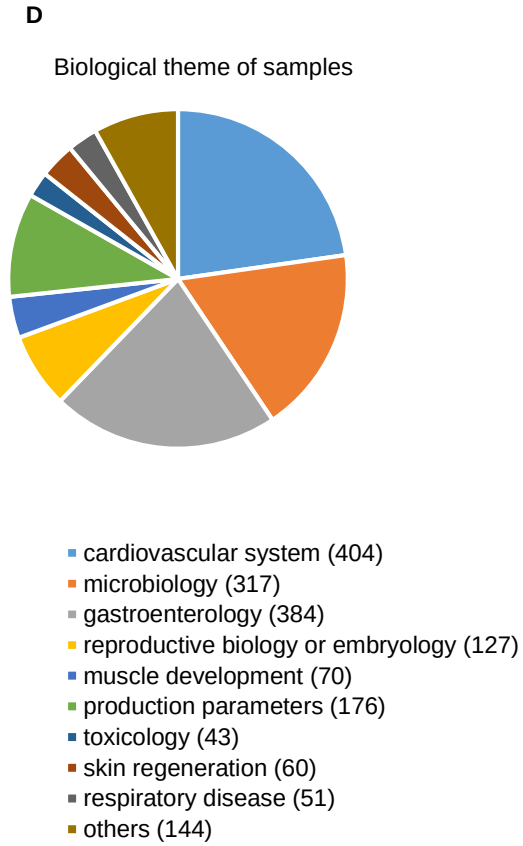
D
Biological theme of samples
cardiovascular system (404)
microbiology (317)
gastroenterology (384)
reproductive biology or embryology (127)
muscle development (70)
production parameters (176)
toxicology (43)
skin regeneration (60)
respiratory disease (51)
others (144)

Figure 2

A

B PorSignDB performance in lymph nodes of PMWS pigs VS healthy pigs

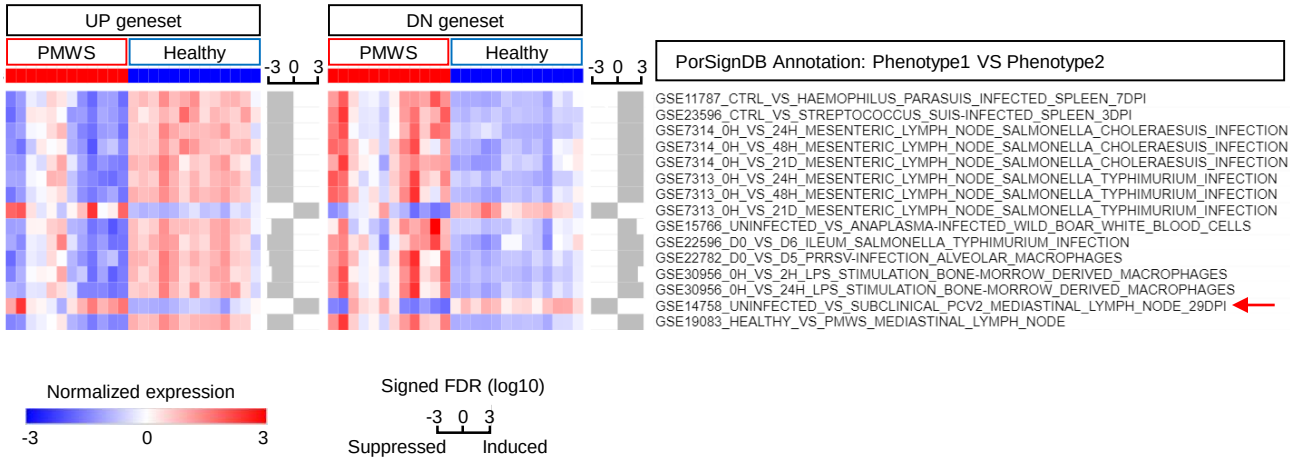

Figure 3

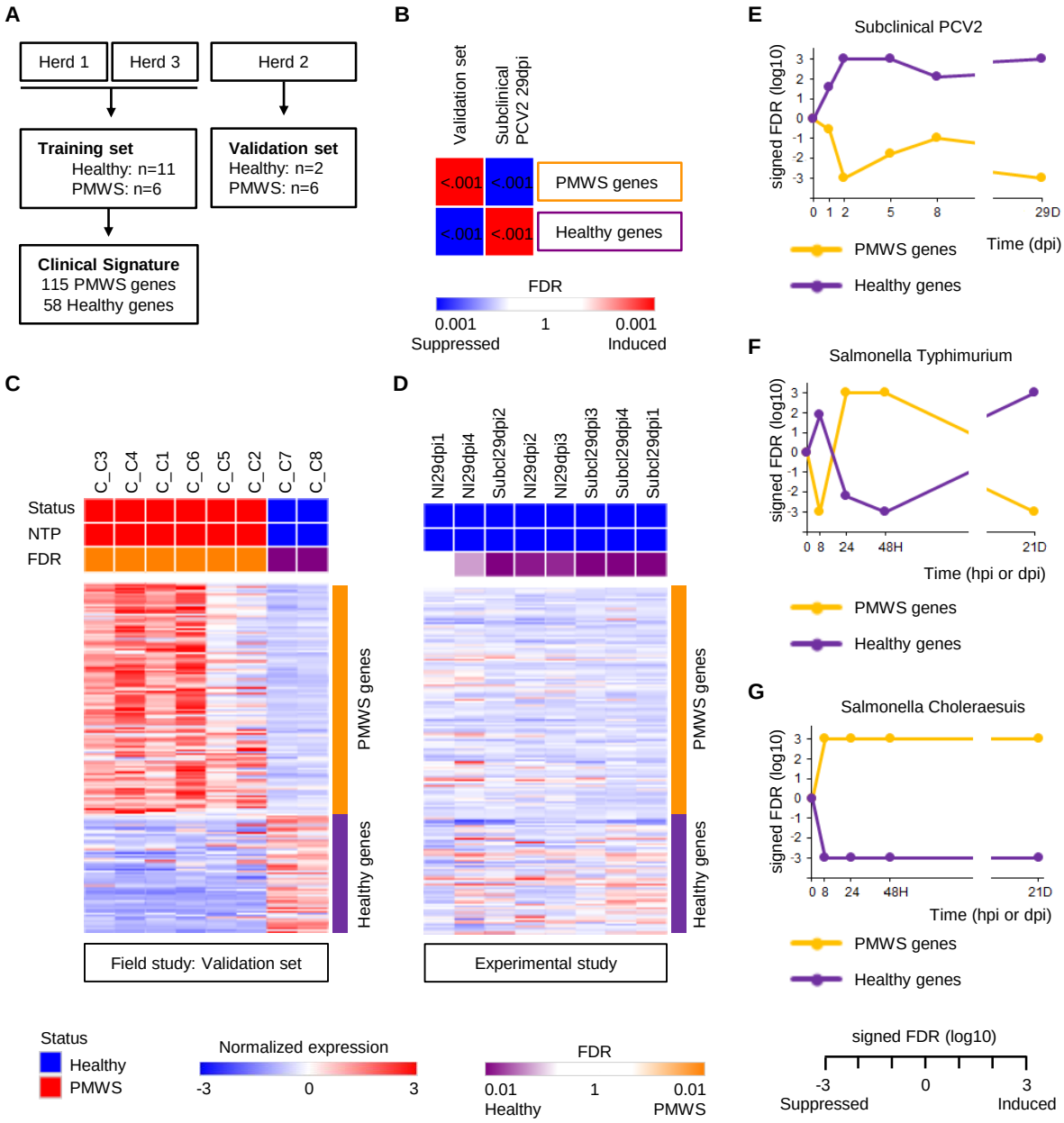
A
Herd 1
Herd 3
Herd 2
Training set
Healthy: n=11
PMWS: n=6
Validation set
Healthy: n=2
PMWS: n=6
Clinical Signature
115 PMWS genes
58 Healthy genes
B
Validation set
Subclinical PCV2 29dpi
<.001
<.001
PMWS genes
<.001
<.001
Healthy genes
FDR
0.001
1
0.001
Suppressed
Induced
C
C_C3
C_C4
C_C1
C_C6
C_C5
C_C2
C_C7
C_C8
Status
NTP
FDR
PMWS genes
Healthy genes
Field study: Validation set
D
NI29dpi1
NI29dpi4
Subcl29dpi2
NI29dpi2
NI29dpi3
Subcl29dpi3
Subcl29dpi4
Subcl29dpi1
PMWS genes
Healthy genes
Experimental study
Status
Healthy
PMWS
Normalized expression
-3
0
3
FDR
0.01
1
0.01
Healthy
PMWS
E
Subclinical PCV2
signed FDR (log10)
0 1 2 5 8 29D
Time (dpi)
PMWS genes
Healthy genes
F
Salmonella Typhimurium
signed FDR (log10)
0 8 24 48H 21D
Time (hpi or dpi)
PMWS genes
Healthy genes
G
Salmonella Choleraesuis
signed FDR (log10)
0 8 24 48H 21D
Time (hpi or dpi)
PMWS genes
Healthy genes
signed FDR (log10)
-3
0
3
Suppressed
Induced

Figure 4

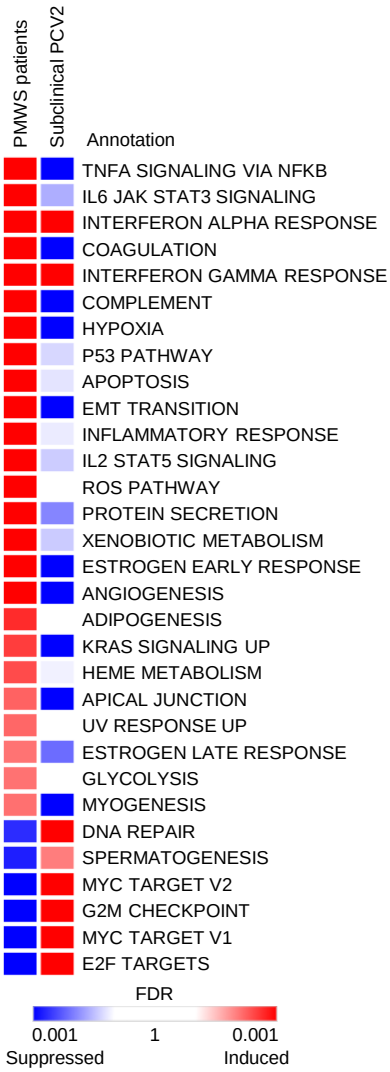
PMWS patients
Subclinical PCV2
Annotation
TNFA SIGNALING VIA NFKB
IL6 JAK STAT3 SIGNALING
INTERFERON ALPHA RESPONSE
COAGULATION
INTERFERON GAMMA RESPONSE
COMPLEMENT
HYPOXIA
P53 PATHWAY
APOPTOSIS
EMT TRANSITION
INFLAMMATORY RESPONSE
IL2 STAT5 SIGNALING
ROS PATHWAY
PROTEIN SECRETION
XENOBIOTIC METABOLISM
ESTROGEN EARLY RESPONSE
ANGIOGENESIS
ADIPOGENESIS
KRAS SIGNALING UP
HEME METABOLISM
APICAL JUNCTION
UV RESPONSE UP
ESTROGEN LATE RESPONSE
GLYCOLYSIS
MYOGENESIS
DNA REPAIR
SPERMATOGENESIS
MYC TARGET V2
G2M CHECKPOINT
MYC TARGET V1
E2F TARGETS
FDR
0.001
1
0.001
Suppressed
Induced

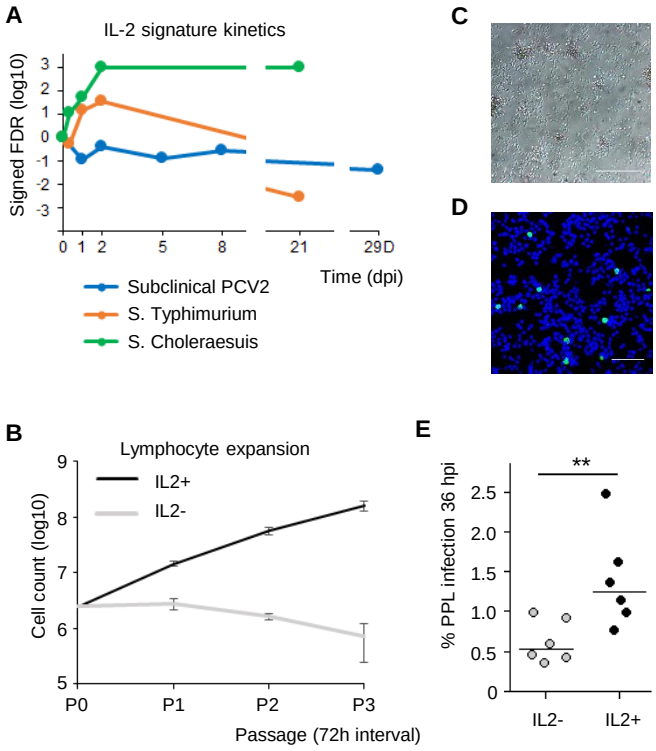
A
IL-2 signature kinetics
Signed FDR (log10)
3
2
1
0
-1
-2
-3
0 1 2 5 8 21 29D
Time (dpi)
Subclinical PCV2
S. Typhimurium
S. Choleraesuis
C
D
B
Lymphocyte expansion
IL2+
IL2-
Cell count (log10)
9
8
7
6
5
P0 P1 P2 P3
Passage (72h interval)
E
**
% PPL infection 36 hpi
2.5
2.0
1.5
1.0
0.5
0
IL2- IL2+

Figure 6

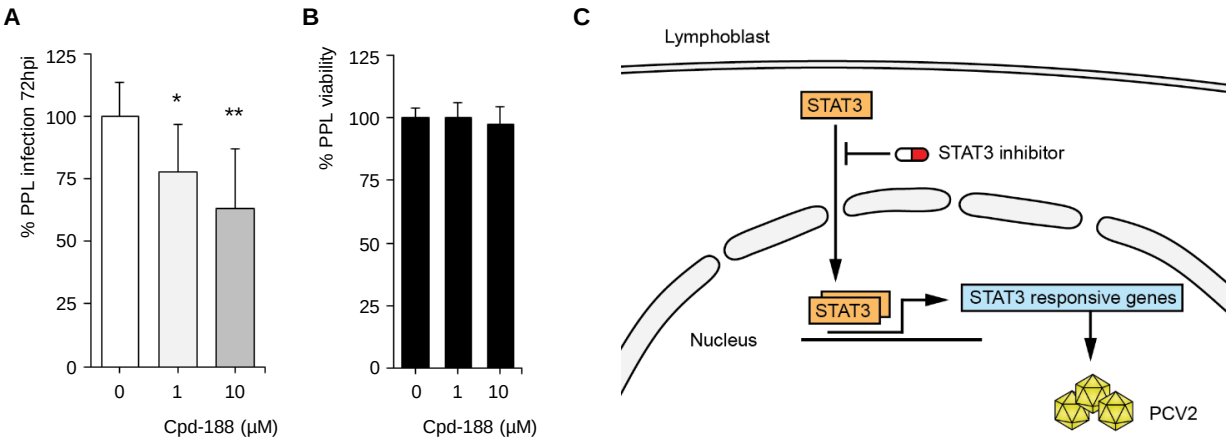
A
% PPL infection 72hpi
125
100
75
50
25
0
*
**
0
1
10
Cpd-188 (µM)
B
% PPL viability
125
100
75
50
25
0
0
1
10
Cpd-188 (µM)
C
Lymphoblast
STAT3
STAT3 inhibitor
STAT3
STAT3 responsive genes
Nucleus
PCV2

Figure 7

A

ImmuneSigDB performance in lymph nodes of PMWS pigs VS healthy pigs

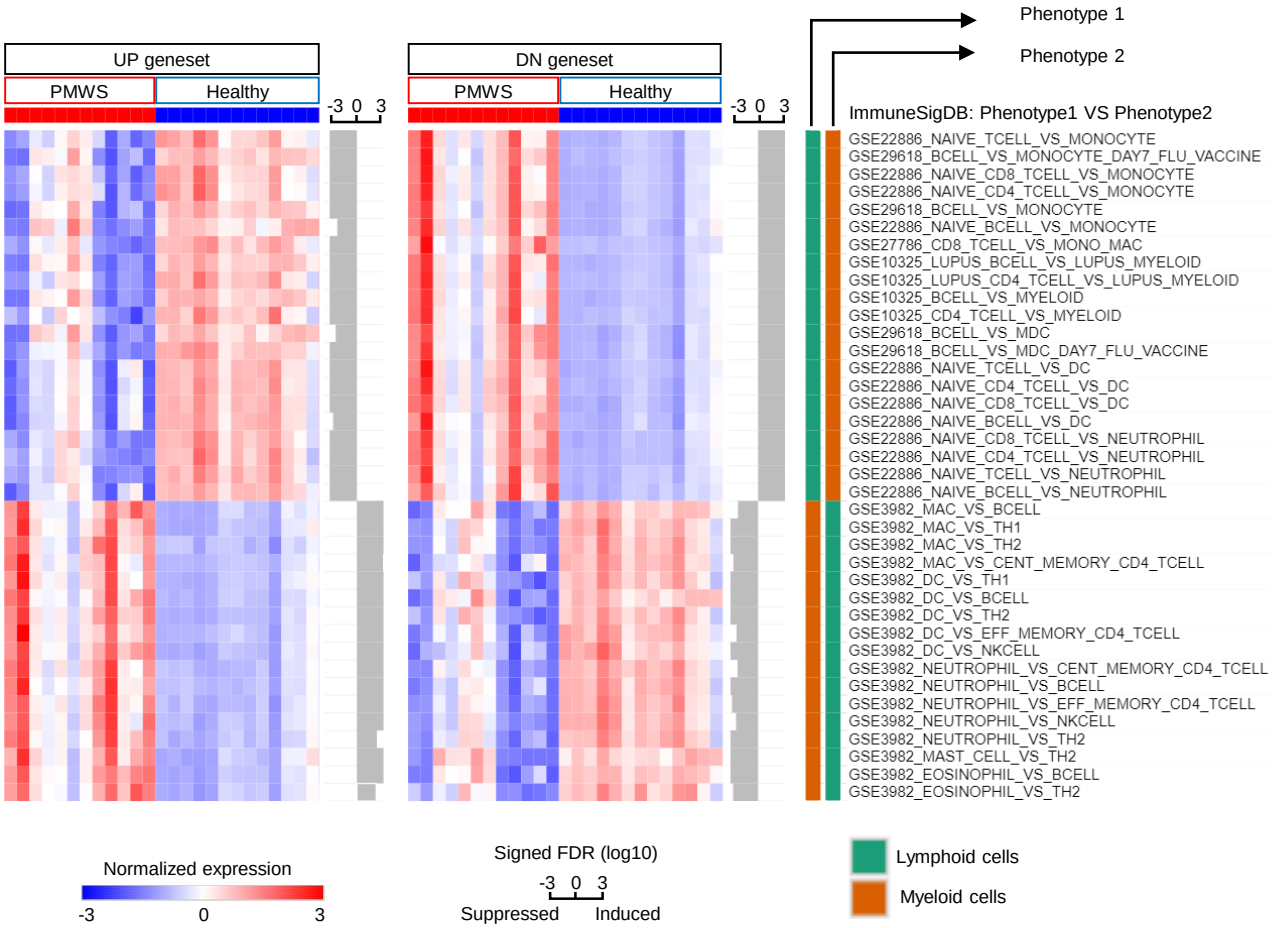

B

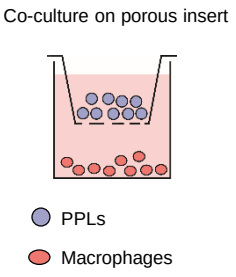

C

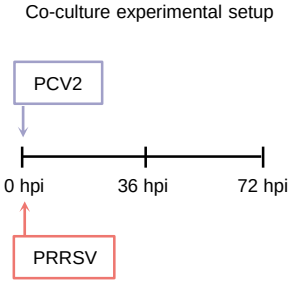

D

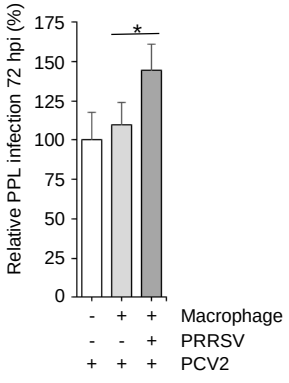

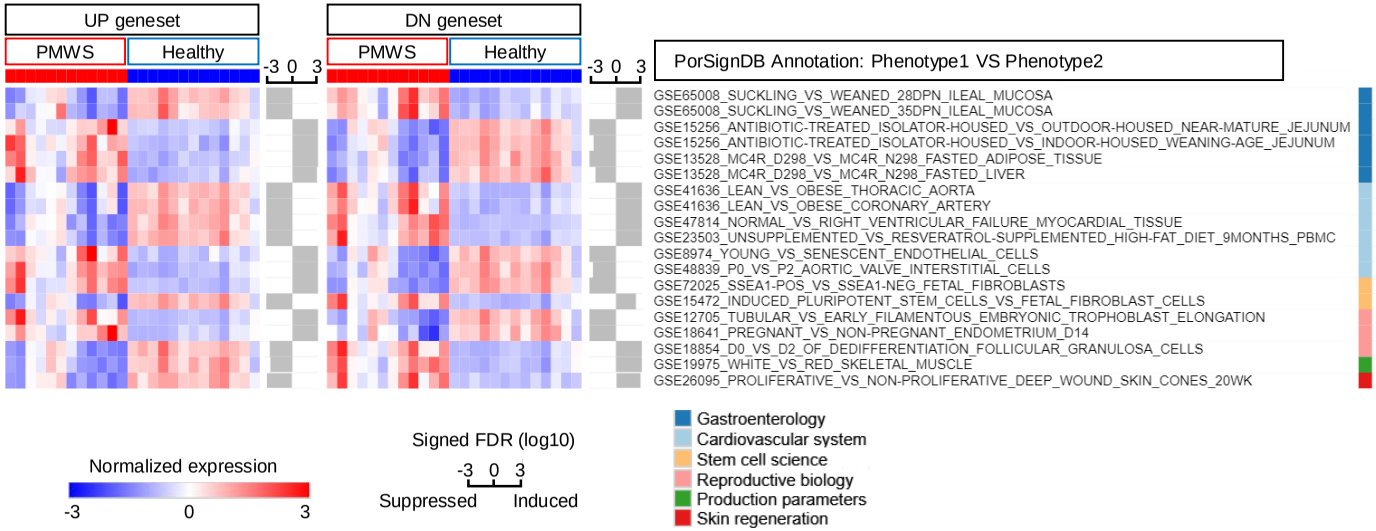
UP geneset
PMWS
Healthy
-3 0 3
DN geneset
PMWS
Healthy
-3 0 3
PorSignDB Annotation: Phenotype1 VS Phenotype2
GSE65008_SUCKLING_VS_WEANED_28DPN_ILEAL_MUCOSA
GSE65008_SUCKLING_VS_WEANED_35DPN_ILEAL_MUCOSA
GSE15256_ANTIBIOTIC-TREATED_ISOLATOR-HOUSED_VS_OUTDOOR-HOUSED_NEAR-MATURE_JEJUNUM
GSE15256_ANTIBIOTIC-TREATED_ISOLATOR-HOUSED_VS_INDOOR-HOUSED_WEANING-AGE_JEJUNUM
GSE13528_MC4R_D298_VS_MC4R_N298_FASTED_ADIPOSE_TISSUE
GSE13528_MC4R_D298_VS_MC4R_N298_FASTED_LIVER
GSE41636_LEAN_VS_OBESE_THORACIC_AORTA
GSE41636_LEAN_VS_OBESE_CORONARY_ARTERY
GSE47814_NORMAL_VS_RIGHT_VENTRICULAR_FAILURE_MYOCARDIAL_TISSUE
GSE23503_UNSUPPLEMENTED_VS_RESVERATROL-SUPPLEMENTED_HIGH-FAT_DIET_9MONTHS_PBMC
GSE8974_YOUNG_VS_SENESCENT_ENDOTHELIAL_CELLS
GSE48839_P0_VS_P2_AORTIC_VALVE_INTERSTITIAL_CELLS
GSE72025_SSEA1-POS_VS_SSEA1-NEG_FETAL_FIBROBLASTS
GSE15472_INDUCED_PLURIPOTENT_STEM_CELLS_VS_FETAL_FIBROBLAST_CELLS
GSE12705_TUBULAR_VS_EARLY_FILAMENTOUS_EMBRYONIC_TROPHOBLAST_ELONGATION
GSE18641_PREGNANT_VS_NON-PREGNANT_ENDOMETRIUM_D14
GSE18854_D0_VS_D2_OF_DEDIFFERENTIATION_FOLLICULAR_GRANULOSA_CELLS
GSE19975_WHITE_VS_RED_SKELETAL_MUSCLE
GSE26095_PROLIFERATIVE_VS_NON-PROLIFERATIVE_DEEP_WOUND_SKIN_CONES_20WK
Normalized expression
-3 0 3
Signed FDR (log10)
-3 0 3
Suppressed Induced
Gastroenterology
Cardiovascular system
Stem cell science
Reproductive biology
Production parameters
Skin regeneration

Figure S1

Figure S2

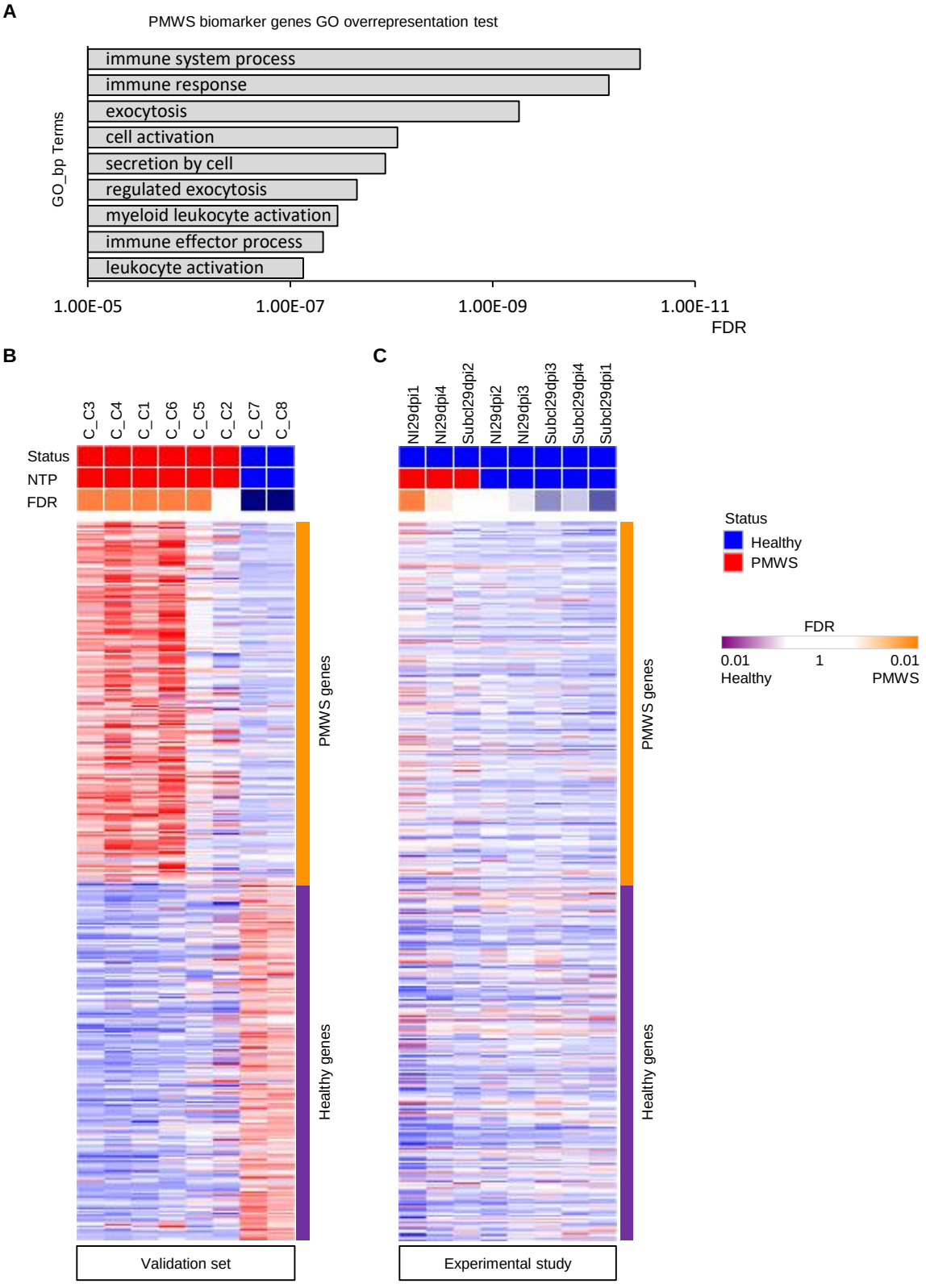
A
PMWS biomarker genes GO overrepresentation test
GO_bp Terms
immune system process
immune response
exocytosis
cell activation
secretion by cell
regulated exocytosis
myeloid leukocyte activation
immune effector process
leukocyte activation
1.00E-05
1.00E-07
1.00E-09
1.00E-11
FDR
B
C_C3
C_C4
C_C1
C_C6
C_C5
C_C2
C_C7
C_C8
Status
NTP
FDR
PMWS genes
Healthy genes
Validation set
C
NI29dpi1
NI29dpi4
Subcl29dpi2
NI29dpi2
NI29dpi3
Subcl29dpi3
Subcl29dpi4
Subcl29dpi1
PMWS genes
Healthy genes
Experimental study
Status
Healthy
PMWS
FDR
0.01
Healthy
1
0.01
PMWS

Figure S3

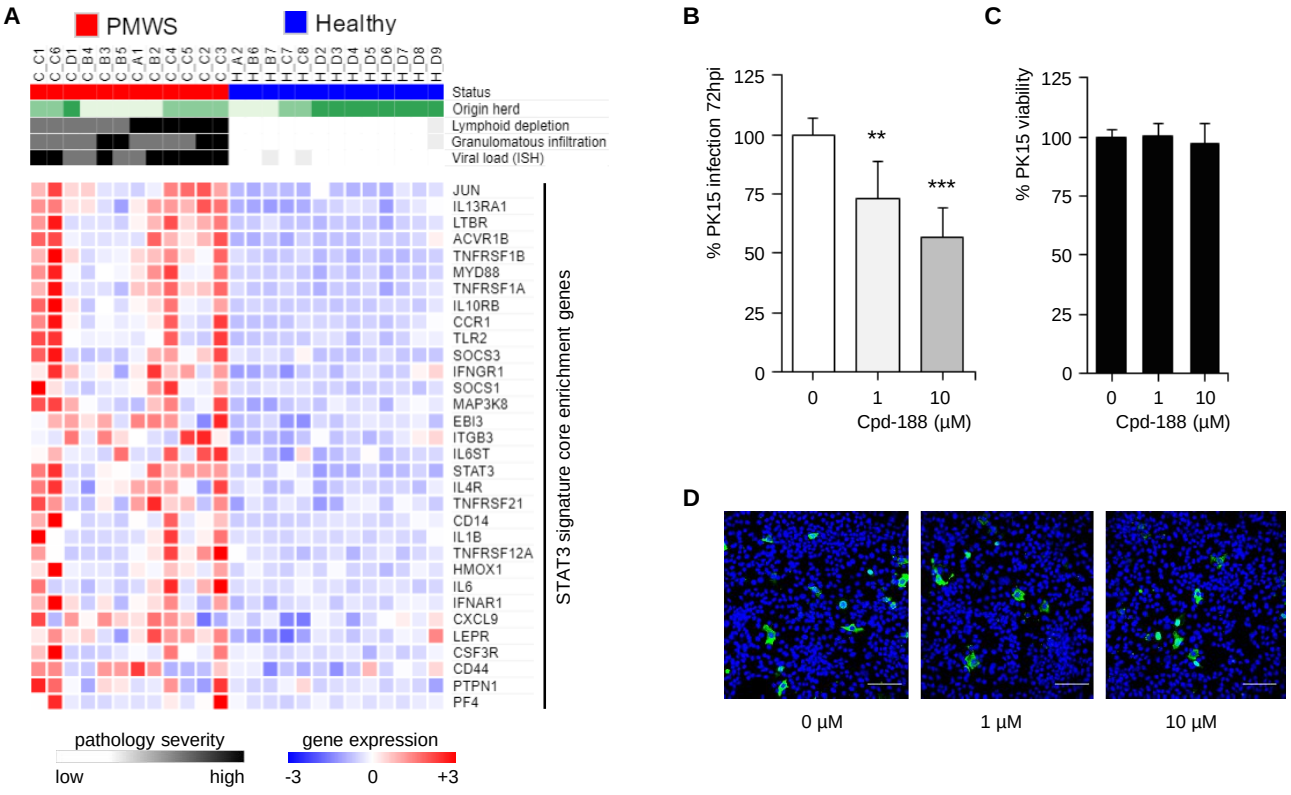
A
PMWS
Healthy
C_C1 C_C6 C_D1 C_B4 C_B3 C_B5 C_A1 C_B2 C_C4 C_C5 C_C2 C_C3 H_A2 H_B6 H_B7 H_C7 H_C8 H_D2 H_D3 H_D4 H_D5 H_D6 H_D7 H_D8 H_D9
Status
Origin herd
Lymphoid depletion
Granulomatous infiltration
Viral load (ISH)
JUN
IL13RA1
LTBR
ACVR1B
TNFRSF1B
MYD88
TNFRSF1A
IL10RB
CCR1
TLR2
SOCS3
IFNGR1
SOCS1
MAP3K8
EBI3
ITGB3
IL6ST
STAT3
IL4R
TNFRSF21
CD14
IL1B
TNFRSF12A
HMOX1
IL6
IFNAR1
CXCL9
LEPR
CSF3R
CD44
PTPN1
PF4
STAT3 signature core enrichment genes
pathology severity
low
high
gene expression
-3
0
+3
B
% PK15 infection 72hpi
125
100
75
50
25
0
**
***
0
1
10
Cpd-188 (μM)
C
% PK15 viability
125
100
75
50
25
0
0
1
10
Cpd-188 (μM)
D
0 μM
1 μM
10 μM